ОБЪЕДИНЕННЫЙ
ИНСТИТУТ
ЯДЕРНЫХ
ИССЛЕДОВАНИЙ

Дубна

E13 - 4697

L.Ondriš, S.V.Richvickij, I.N.Semenyushkin,
P.Horvath, A.N.Khrenov

ЛАБОРАТОРИЯ ВЫСОКИХ ЭНЕРГИЙ

FAST TIMING CIRCUIT USING A CHARGE STORAGE DIODE

1969

E13 - 4697

L.Ondriš, S.V.Richvickij, I.N.Semenyushkin,
P.Horvath, A.N.Khrenov

FAST TIMING CIRCUIT USING A CHARGE STORAGE DIODE

Submitted to "Nucl. Instruments and Methods".

Introduction

In some papers the best conditions for high time resolution of the photomultiplier counter pulse timing have been well established[1,2,3,4]. Various circuits for the timing of the scintillation counter pulses are also designed. The problem of the time shift, caused by the different amplitudes of the input pulses, has been solved in these circuits practically by two ways: by the use of the zero crossing technique and by the use of the time shift compensation[5,6,7,8,9, 10].

The described circuit relates to the last one and it was designed for the use in some experiments in high energy physics.

Method

The time shift compensation, based on the charge storage effect in diodes, was used. A block diagram of the circuit is shown in Fig.1. The bipolar photomultiplier pulse (Fig.2) is applied to two discriminators D_1, D_2 and they trigger two fast current generators $i_1(t)$, $i_2(t)$. The negative part of the bipolar pulse triggers the current generator $i_1(t)$ at the time t_0. This time t_0 depends on the D_1 discriminator level U_{D_1} and on the pulse amplitude. During the time interval, when the waveform of the bipolar pulse is rising and becomes positive, the current generator $i_2(t)$ is triggered at the time $T_0 + t_0'$, where T_0 is the time of the "zero crossing point".

Figure 2 also shows the approximative waveform of the bipolar scintillation pulse (dashed curve), composed of straight lines. For this approximative waveform the ratio of t_0' and t_0 as a function of the bipolar pulse amplitude is constant :

$$\frac{t_0'}{t_0} \approx k . \qquad (1)$$

For the real bipolar pulse this equation is also valid in the defined pulse amplitude region.

The currents $i_1(t)$ and $i_2(t)$ are applied to the charge storage diode so, that the diode goes to the forward conduction state at first. When the total diode current $i(t) = i_1(t) + i_2(t)$ became reverse, the diode resistance remains low as long as the stored charge is not completely removed. At the instant t_{off}, when the diode resistance is rapidly increased, the output discriminator D_3 is triggered.

Up to this time t_{off} the stored charge in the diode can be approximately described by the equation:

$$\frac{dq}{dt} + \frac{q}{\tau} = i(t) , \qquad (2)$$

where q is the stored charge, $i(t)$ is the total diode current, τ is the lifetime of the minority carriers.

The calculation of the time t_{off} from eq. (2) for the real charge and discharge current waveforms $i_1(t)$ and $i_2(t)$ practically is impossible. But this is quite easy, when charge and discharge currents are formed by the step functions or by the ramp functions. These approximative waveforms serve especially for a qualitative description of processes, in the charge storage diode connected in real circuite, but to achieve such waveforms of current pulses in real circuits is impossible.

At first, the case of $\tau \gg T_0$ is given.

Table 1 presents the charge and discharge current waveforms and results of the t_{off} calculation.

We see that t_{off} is independent of t_0 and therefore also of the amplitude of the input bipolar pulse for the defined relation between k and $\frac{I_1}{I_2}$. These relations are also shown in Table 1. By adjusting the ratio $\frac{I_1}{I_2}$ of charge and discharge current amplitudes, one can obtain the optimum amplitude time shift compensation, e.g. t_{off} = const.

As an example for τ of the order of T_0, the functions $t_{off} = f(U_1)$, calculated from eq.(2), are shown in Fig.3. U_1 is the amplitude of the scintillation pulse. The charge and discharge currents were as in Table 1a.

In the described circuit, where charge and discharge currents of the diode are more real waveforms, the adjusting of the optimum amplitude time shift compensation by the ratio of $\frac{I_1}{I_2}$ is also possible.

Description of the Circuit

The complete circuit is shown in Fig.4. The discriminator D_1 and the current generator $i_1(t)$ triggered by the negative part of the bipolar pulse are composed of the diodes TD_1, BD_1 and the transistors T_1, T_2. The discriminator D_2 and the current generator $i_2(t)$ triggered by the positive part of the bipolar pulse are composed of the diodes TD_2, BD_2, BD_3 and the transistors T_3, T_4 /11/. The charge and discharge current ratio is adjustable by the potentiometer P_3. The diode 2D503 was used as the charge storage diode. The diodes TD_3, BD_4, BD_5 and the transistor T_5 form the output circuit. The output pulse is negative, of a 0.5 V pulse height, 15 ns wide and of 2 ns rise-time and fall-time.

Results

The experimental arrengement for the time shift measurement is shown in Fig.5.

The amplitude of photomultiplier output pulses was adjusted by the polarizing filter and the time shift of the fast timing circuit was measured by a time-to-pulse height converter and a multichannel analyser. Figure 6 shows the time shift as a function of the input pulse amplitude. The result better than $\pm$140 ps time shift within the 0.09-10 V and $\pm$70 ps within the 0.6-10 V input pulse amplitude range was achieved.

The photomultiplier and fast timing circuits were tested in the 5 GeV π^--meson beam. The π^--meson time-of-flight between the two scintillation counters was measured. Plastic scintillators 25 x 25 x 25 mm and XP 1020 photomultipliers were used. A time resolution full width at half maximum of 0.33 ns was obtained, the channel width being 140 ps.

The overall time resolution curves (A) and (B) are shown in Fig.7. The second curve (B) was measured, after the 2 ns time delay had been inserted. A time resolution of 0.6 ns (curve (C)) was obtained with a standard timing circuit, without the time shift compensation.

Referencess

1. E.Gatti, V.Svelto. Nucl. Instrum. & Meth., 43, 1, 248 (1966).
2. L.G.Hyman, R.M.Schwarcz, R.A.Shulter. Rev. Sci.Instr., 35, 3, 393 (1964).
3. L.G.Hyman. Rev. Sci. Instr., 36, 7, 193 (1955).
4. G.Bertolini, M.Cochi, V. Mandi, A.Rota. IEEE Transactions N.S. - 13, 3, 119 (1966).
5. B.M. Shoffner, E.E.Shrader. IEEE Transactions N.S. -13, 1, 394 (1966).
6. J.K.Whittaker. IEEE Transactions N.S. - 13, 1 , 199 (1966).
7. Donald L.Wieber, Harlan W.Lefevre. IEEE Transactions N.S.- 13, 1, 389 (1966).
8. J.Grunberg, L.Tepper. IEEE Transactions N.S. - 13, 1, 389(1966)
9. V.G.Lapshin, V.I.Rykalin, Z.Cisek. JINR Preprint 13-3530, Dubna., 1967.
10. D.A. Gedcke, W.J.McDonald. Nucl. Instrum. & Meth. 58, 253(1968).
11. H.Verweij. Conference on Nucl. Electronics, Paris , 1963.

Received by Publishing Department
on September 5, 1969.

Table 1

The charge and discharge current waveforms and results of the calculation

	$i_1(t)$, $i_2(t)$	$\frac{t_{off}}{T_0} = f\left(\frac{t_0}{T_0}\right)$	$t_{off} = const$
(a)	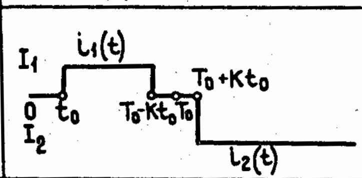	$\frac{t_{off}}{T_0} = 1 + \frac{I_1}{I_2} + \frac{t_0}{T_0}\left[K-(1-K)\frac{I_1}{I_2}\right]$	$\frac{I_1}{I_2} = \frac{K}{1+K}$
(b)	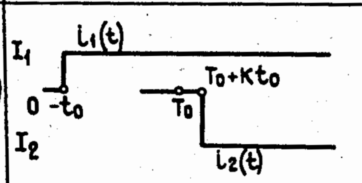	$\frac{t_{off}}{T_0} = 1 + \frac{1}{\frac{I_2}{I_1}-1} + \frac{t_0}{T_0}\left[K-(1-K)\frac{1}{\frac{I_2}{I_1}-1}\right]$.	$\frac{I_1}{I_2} = K$
(c)	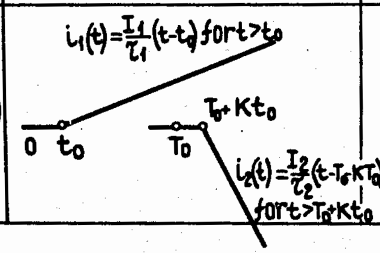	$\frac{t_{off}}{T_0} = 1 + \frac{1}{\sqrt{\frac{I_2}{I_1}}-1} + \frac{t_0}{T_0}\left[K-(1-K)\frac{1}{\sqrt{\frac{I_2}{I_1}}-1}\right]$	$\frac{I_1}{I_2} = K^2$

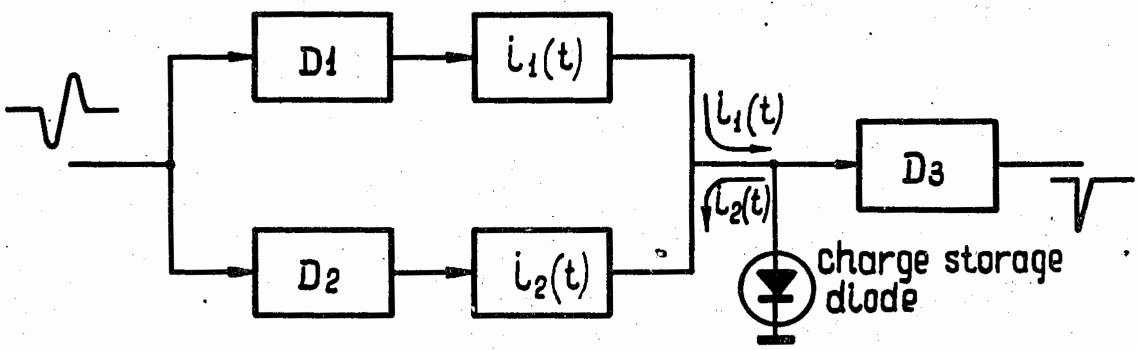

Fig.1. A block diagram of the fast timing circuit. D_1, D_2, D_3 – discriminators; $i_1(t)$, $i_2(t)$ – current generators.

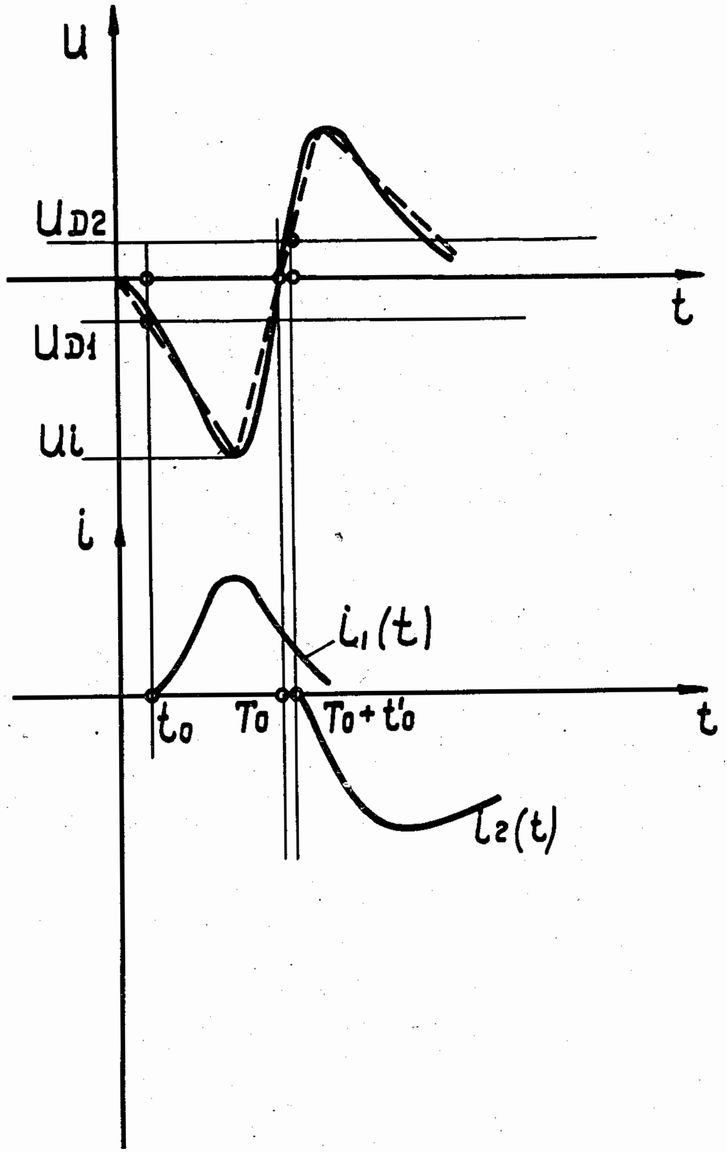

Fig.2. The bipolar photomultiplier pulse and current pulses $i_1(t)$, $i_2(t)$.

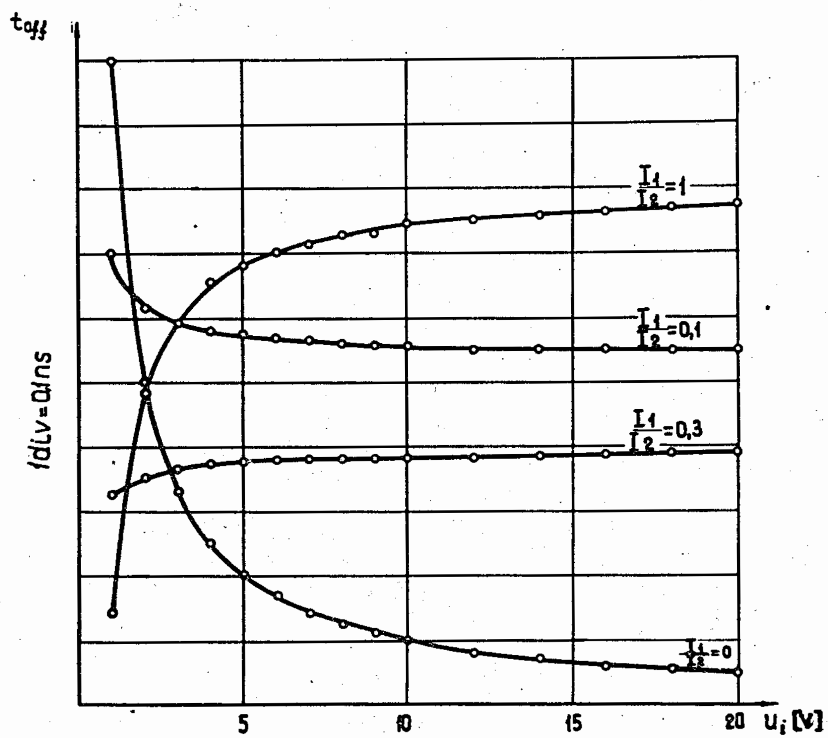

Fig.3. Calculated functions $t_{off} = f(U_i)$ for τ = 5 ns, T_0 = 3.4 ns, U_{D_1} = 0.5 V, U_{D_2} = 0.2 V, k = 0.28.

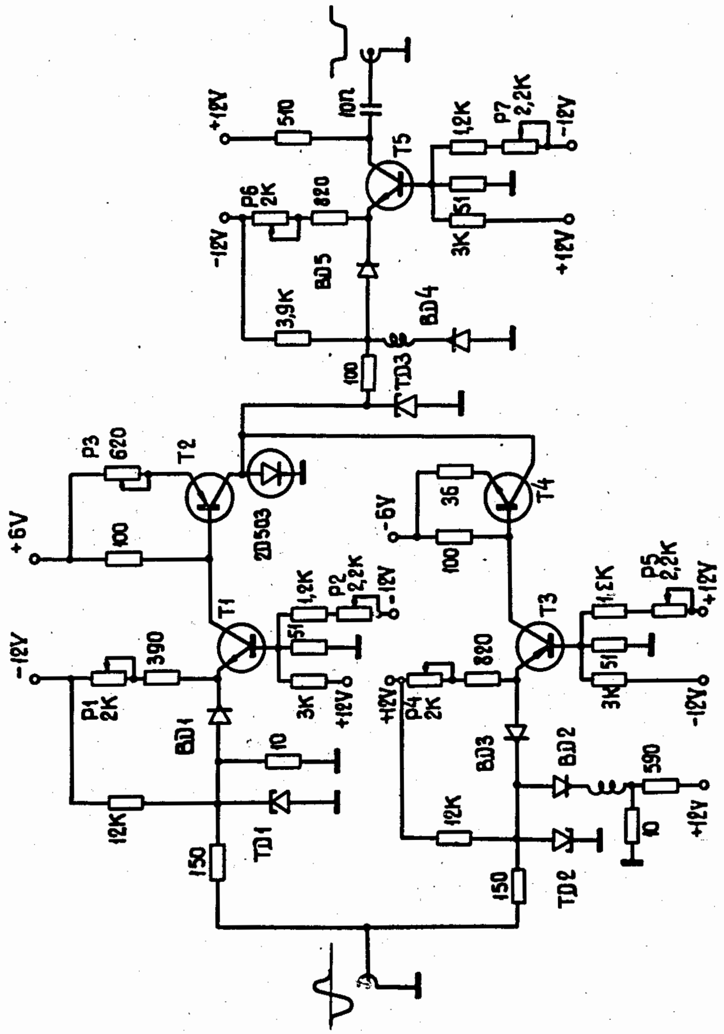

Fig.4. A circuit diagram for the fast timing circuit.

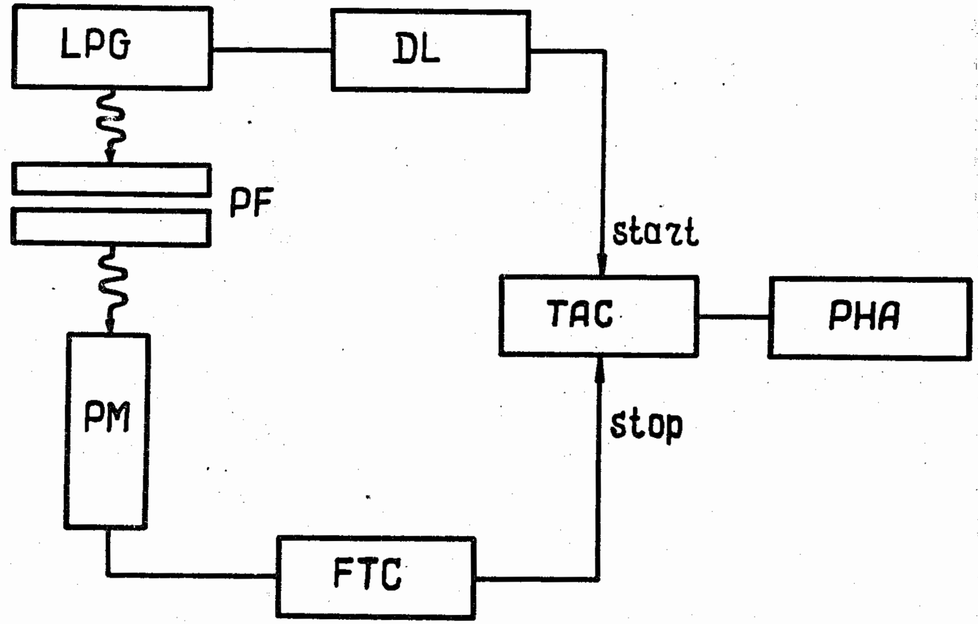

Fig.5. The experimental arrangement for the amplitude time shift measurement. LPG - light pulse generator; PM - photomultiplier; PF - polarizing filters; FTC - fast timing circuit; DL - delay line; TAC - time-to-pulse height converter; PHA - pulse height analyzer.

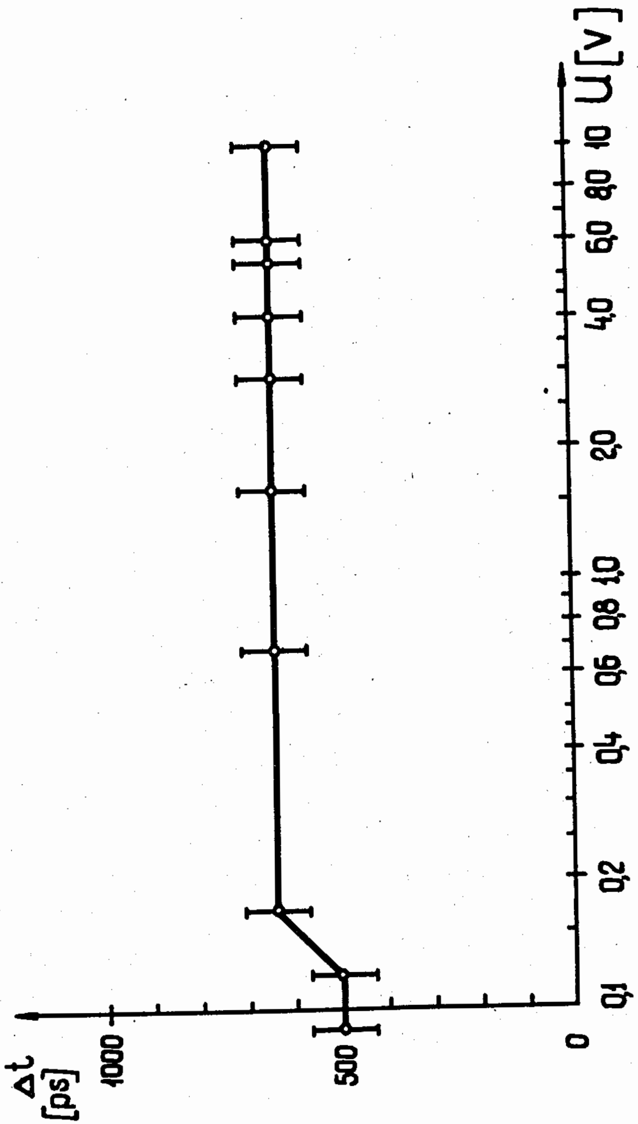

Fig. 6. The time shift of the output pulse as a function of the input pulse amplitude.

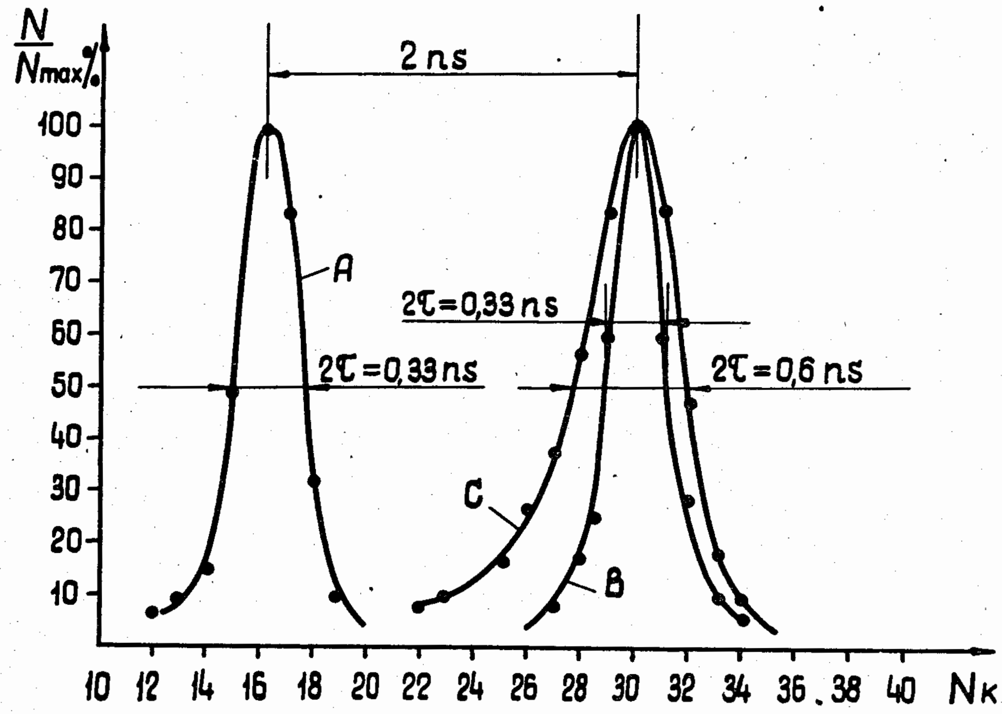

Fig.7. The overall time resolution curves.